

Development of Breakup Model for Large Eddy Simulation of Diesel Spray

Koji Kitaguchi, Soichi Hatori, Tsukasa Hori, Jiro Senda^{*}
Mechanical Engineering Department, Doshisha University, Japan
jsenda@mail.doshisha.ac.jp

Abstract

Large Eddy Simulation (LES) has been applied for non-evaporative diesel spray, evaporative diesel sprays and diesel spray flame in earlier studies. As a result, LES analyses can be simulated 3D vortex structure. However, spray droplet diameter and spray shape of LES analyses are not appropriate in the comparison with the experimental results. This is because breakup model is not appropriate for LES. Diesel spray is injected with high pressure. So, breakup caused by shearing force is dominant at upper stream region of spray. The downstream region of spray is corresponding to relatively low Weber number condition due to the momentum exchange with ambient gas. Thus, Kelvin-Helmholtz (KH) model and Modified Taylor Analogy Breakup (MTAB) model are used for primary and secondary breakup processes respectively. This study is focused on the development of breakup model. LES of non-evaporating diesel spray are performed using KHRT model, MTAB model and KH-MTAB model. Then, LES with these models were compared with experimental results. As a result, the availability of KH-MTAB model is showed. It is found that KH-MTAB is good agreement with experimental results.

Introduction

Diesel engines emit soot and nitrogen oxide (NO_x). The formation of these emissions is affected by heterogeneous distribution in diesel spray. This heterogeneous distribution is affected by turbulent vortex structure. Thus, the high accuracy prediction for the amount of these emissions needs to estimate finer turbulent vortex structure.

Reynolds Averaged Navier-Stokes (RANS) is used as turbulent analysis method. This is effective to get an averaged value, which is important in design, with low computational cost, but the computational results highly depend on the turbulent model, such as k - ϵ , RNG k - ϵ , Reynolds Stress Model (RSM). Furthermore, the model constants need to be optimized with respect to each computational objective in order to improve prediction accuracy. This is because universal characteristics in the three dimensional turbulent flow structures cannot be described extensively enough. To overcome this issue, Large Eddy Simulation (LES) has been expected as an alternative approach to RANS [1]. In LES, vortex components of flow field are divided into large scale and small scale based on the computational cell. The large scale motion is calculated directly, while small scale is modeled with a Sub Grid Scale (SGS) model. LES can predict large scale vortex structures of the turbulent flow field in the spray. Thus, LES can reproduce the universal characteristics of turbulent flow structure when we use a finer computational grid.

The authors applied LES for diesel spray simulation using KIVALES, a LES model incorporated into KIVA code. Simulations have been done for non-evaporative, evaporative spray, and spray combustion [1-3]. In LES, computational grid has a major impact on the calculation result. The results of non-evaporative and evaporative spray with a finer computational grid reproduced unsteady and 3-D vortex structure using LES [2]. Spray characteristics such as sauter mean diameter and spray shape does not match with the experimental results.

In this paper, breakup model has been developed to confirm the spray characteristic to experiment results. First, we examined the effect of breakup model under relatively low density conditions. After that, validation under the relatively high ambient density is conducted in order to simulate the high density condition corresponding to top-dead center of supercharging and high EGR diesel engines.

Numerical Methods [4-7]

The governing equations used in KIVA-LES are continuous, momentum, internal energy equation and chemical species equations. The filter used in this study is a top-hat filter. As it is usual for the simulations of compressible turbulence, we employ Favre-filtering. The diffusion of a physical quantity is used a gradient diffusion model.

SGS stress model is k - Δ model which modelled by turbulence energy k^{sgs} in SGS and computational grid width Δ . In addition, the SGS scalar model is gradient diffusion model.

The fuel spray is modeled using Discrete Droplet Model (DDM). Blobs model is applied to fuel injection so that fuel droplet diameter injected from injector is equivalent to the nozzle diameter. The number of parcels is

^{*}Jiro Senda jsenda@mail.doshisha.ac.jp

40,000 per one injection. Effect of internal flow in nozzle is not considered. Collision and coalescence of droplet in the spray is not considered. Velocity variation of droplet in the spray is calculated by momentum equation. To calculate the drag coefficient, $C_{D,sphere}$ was assumed as rigid sphere of droplet:

$$C_{D,sphere} = \begin{cases} \frac{24}{Re_l} (1 + (1/6) Re_l^{2/3}) & Re_l < 1000 \\ 0.424 & Re_l > 1000. \end{cases} \quad (1)$$

However, when using MTAB model is used Liu et al. equation [8] which take into account distortion of droplet.

$$C_D = C_{D,sphere} (1 + 2.632y). \quad (2)$$

In this research, central difference is used on the space derivative of convective term in momentum equation. The other space derivatives of convective terms are calculated using Quasi-Second Order Upwind (QSOU) method filled with monotonicity and stability. For the sub-cycle, 4th-order Runge-Kutta method is used on the time derivative of convective term in momentum equation. The other time derivatives of convective terms are calculated using forward Euler's rule.

Figure 1 shows the computational grid in this report. The computational domain is the cylinder with diameter of 30 mm and height of 100mm. Since this research is focused on free spray, computational domain can be smaller than experimental domain, in order to reduce the computational time. The computational grids are 60 in radial direction, 60 in circumferential direction and 200 in height with a total of 720,000 grids. All boundaries of the computational grids are set to non-slip wall. The initial flow in the computational domain is in quiescent state. The injection point is set to the center of the upper surface, and the injection direction is downward. Time step is $1\mu s$, and then the automatic control by KIVA.

Numerical and Experimental Conditions

Table 1 and 2 shows computational conditions of relatively low and high ambient density condition, respectively. The high ambient density condition shown in Table 2 is to simulate the fuel spray injected at top-dead center of supercharging and high EGR diesel engines. In high density conditions, it is difficult to measure the particle size of the entire area of spray, because spray dose not spread enough. Therefore particle size is measured at only pilot spray conditions, which is easy to measure droplet size for relatively low number density of spray droplets by using the super high spatial resolution photography (SHSRP) [9]. SHSRP is the very high resolution measurements system which has both of a high spatial resolution and a wide measurement area developed by our teams. This system has the spatial resolution of $7.8\mu m$.

Figure 2 shows the injection velocity profile measured by spray momentum method at each condition. If given in the injection rate waveform obtained from the experiment, the calculations become unstable. Therefore must be finer the time step, computational cost is significantly increased. Condition of pilot spray is considered the effect of injection rate waveform, given the injection velocity profile obtained from experiment. Any other conditions, injection velocity were constant during injection period.

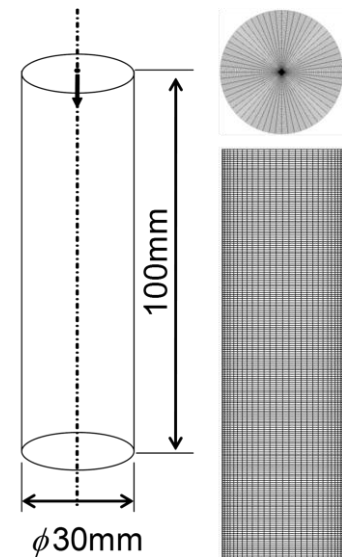


Figure 1 Computational domain

Table 1 Computational and experimental condition for low ambient density

Nozzle hole diameter	[mm]	0.20
Injection pressure	[MPa]	77
Injection duration	[ms]	1.42
Fuel		n-tridecane
Injection fuel amount	[mg]	12.0
Fuel temperature	[K]	300
Ambient gas		N ₂
Ambient pressure	[MPa]	1.5
Ambient density	[kg/m ³]	17.3
Ambient temperature	[K]	300

Table 2 Computational and experimental condition for high ambient density

		Main	Pilot
Hole diameter	[mm]	0.20	
Injection pressure	[MPa]	77	
Injection duration	[ms]	1.30	0.45
Fuel		n-tridecane	
Fuel amount	[mg]	12.0	3.72
Fuel temperature	[K]	300	
Ambient gas		CO ₂	
Ambient pressure	[MPa]	1.8, 2.1, 2.4, 2.7	
Ambient density	[kg/m ³]	35.5, 41.6, 48.4, 55.7	
Ambient temperature	[K]	300	

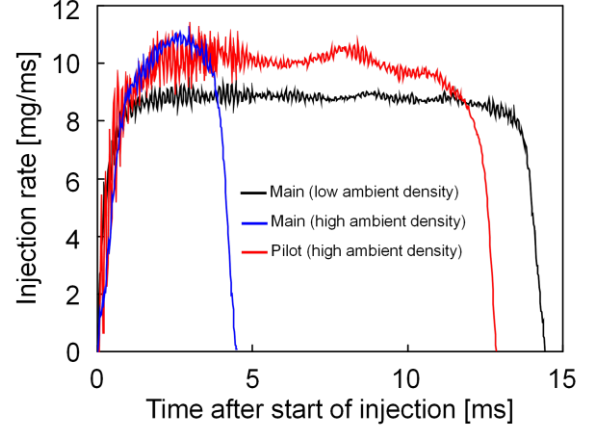


Figure 2 History of injection rate

Breakup model

In this paper, LES calculation was performed to verify the effect of breakup model on the spray characteristics using the Kelvin-Helmholts and Rayleigh-Taylor (a combination of the surface wave instability (KH) model and Rayleigh-Taylor (RT) model : KHRT) model [2], Modified Taylor Analogy Breakup (MTAB) model [10], and KH-MTAB model that is combination of KH [11] model and MTAB model. MTAB model is optimized for the diesel spray simulation with the high injection pressure from Taylor Analogy Breakup (TAB) model [12].

KHRT model is based on breakup regime of comparatively a higher droplet Weber number. On the contrary, MTAB model is based on breakup regime of comparatively a lower Weber number. In the upstream region of diesel spray, breakup is dominated by shear stress, because diesel spray is injected at high pressure. On the other hands, downstream of the spray, breakup is dominated by deformation of the droplet. This is because the momentum of fuel droplets is lost for the momentum exchange with gas phase. We believed that hybrid breakup model of KH model and MTAB model for the primary and secondary breakup is reasonable.

In KH model the generation of child droplets increases the computational cost and it would require a new experimental constant. Therefore, the child droplets are not used. However, the radial momentum after the breakup is added to the parent droplets. In addition, the experimental constant B_I which is necessary to determine the breakup time, employed the 10 for KHRT model and 5 for KH-MTAB model.

Improvement of addition velocity toward radial direction at breakup

In original TAB model [12], droplet radial velocity after breakup is given as following formula:

$$v_{\perp} = C_v C_b r_p \dot{\gamma}, \quad (3)$$

where C_v and C_b are model constants. In the original model, $C_v = 1$ is used from experimental results. Here, $C_b = 0.5$ since the droplet undergoes equal breakup at both sides. However, TAB model has given random droplet radius calculated by χ^2 distribution. It might not be half the radius of the droplet before the breakup. It is important to correctly estimate the representative velocity of the droplet parcel in Discrete Droplet Model (DDM), considering the after breakup droplet mass C_b given as following formula:

$$C_b = \frac{r_p^3 - r_c^3}{r_p^3}. \quad (4)$$

Hybrid model

KHRT model is used with KH model as primary breakup below the breakup length and RT model as secondary breakup beyond the breakup length. Breakup length is defined by Levich theory [13]

$$L_b = C_l d_0 \sqrt{\frac{\rho_f}{\rho_a}}, \quad (5)$$

where d_0 and C_l are the nozzle diameter and the experimental constant, respectively. The value of C_l is given by 5 in this report.

KH-MTAB model uses the KH model for primary breakup at a Weber number $We > 450$ and MTAB model for secondary breakup at $We \leq 450$.

Weber number is given by

$$We = \frac{\rho_g U_r^2 d_p}{\sigma}, \quad (6)$$

where d_p is droplet diameter.

Results and Discussion

Effect of Breakup model

Figure 3 shows local sauter mean diameter (SMD) of LES and experimental result at the end of injection. SMD is calculated as following formula:

$$SMD = \frac{\sum_i (D_i^3 \times N_i)}{\sum_i (D_i^2 \times N_i)}, \quad (7)$$

where D_i is droplet diameter and N_i is droplet number in parcel. SMD in experiment is calculated by applying concentric model to Transmissive Light Extinction Method by Yokota et al [14]. Compared to experiment, KHRT underestimates SMD. MTAB and KH-MTAB agree with the experimental results. As same as Dan's experiment [15], KH-MTAB has a tendency to increase SMD at spray tip; KH model was gradually change the droplet diameter, while MTAB was rapidly changing droplet diameter. Therefore, large droplets go through the central axis of the spray and stay near the spray tip.

Figure 4 shows spray tip penetration by LES and experimental results. Spray tip penetration is defined as axial distance from the nozzle hole to farthest droplets. Spray tip penetration of experiment results are the ensemble average of 5times from shadowgraph photography. The results show that good agreements of MTAB and KH-MTAB were obtained with the experiment, and KHRT underestimated at the end of injection. In KHRT, droplet size is underestimated. As a result the momentum near spray tip is small and KHRT underestimates spray tip penetration.

Figure 5 shows spray volume of LES and experimental results. Spray volume calculation is shown in figure 6. The circular area of the spray volume calculation is divided into 60 identical sections, at each 1mm interval of the spray length. Representative radius is decided by the farthest droplet in each area. Spray volume is also calculated, by circumferential average of representative radius. Experimental results is calculated the ensemble average of 5times from integration in the circumferential direction of the surface area of shadowgraph images. MTAB and KH-MTAB agreed with the experimental results, and KHRT underestimated.

Figure 7 displays temporal change in spray images of LES and experimental results by shadowgraph photography in conditions of $TASI/t_{inj}=0.11, 0.25, 0.5, 1.0, 2.0$. $TASI/t_{inj}$ is dimensionless time, where time after start of injection ($TASI$) is the time from the start of injection normalized by injection period t_{inj} . This figure shows (a) Experimental results, (b) KHRT, (c) MTAB, and (d) KH-MTAB. LES simulates intermittency of spray outline as same as experiment. This phenomenon was more enhanced in KHRT. From the figure 3, KHRT underestimate the droplet diameter. Then droplets tend to follow easy the ambient gas. Compared to experiment, KHRT underestimated the spreading of spray on radial axis at the upstream of spray. In other hands, MTAB and KH-MTAB overestimate it. And compared to MTAB, KH-MTAB estimates the proper spreading of spray on radial axis. At $TASI/t_{inj}=2.0$, KHRT couldn't reproduce the droplet staying near the nozzle. This is considered to be an underestimation of droplet diameter, compared to experiments. On the other hand MTAB and KH-MTAB reproduce the droplet staying near the nozzle.

In consequence good agreement of KH-MTAB model was obtained with experiment in terms of the spray characteristics. In the Next session, spray simulation with KH-MTAB model was conducted for the different ambient density conditions.

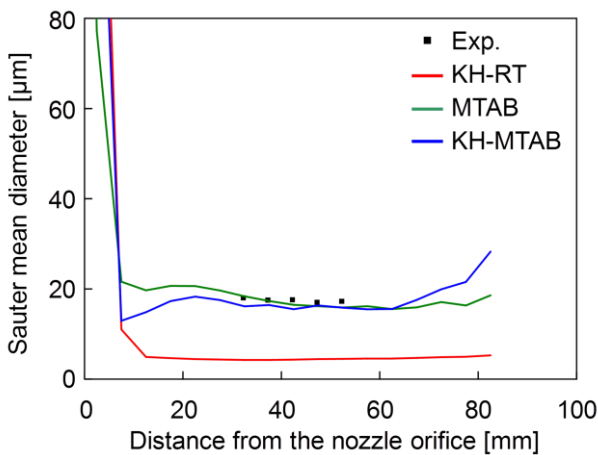


Figure 3 Effects of breakup model on local sauter mean diameter at the time of injection end

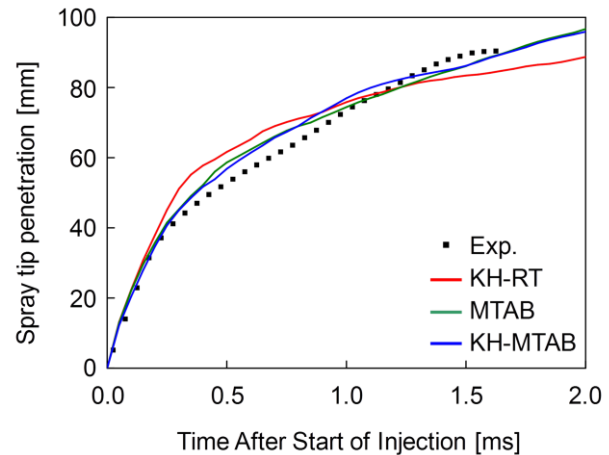


Figure 4 Temporal changes in spray tip penetration as a function of time after start of injection for different breakup model

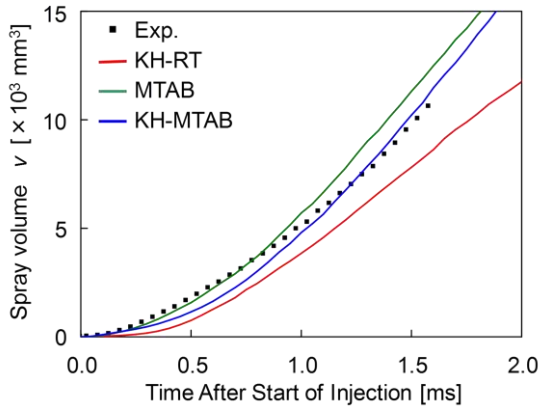


Figure 5 Temporal changes in spray volume as a function of time after start of injection for different breakup model

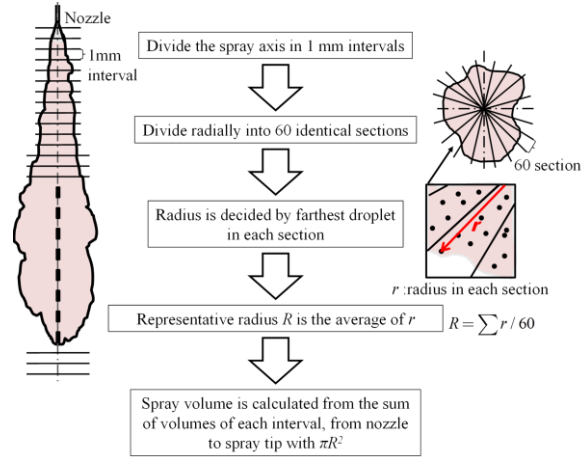


Figure 6 Flowchart of calculate the spray volume and representative radius

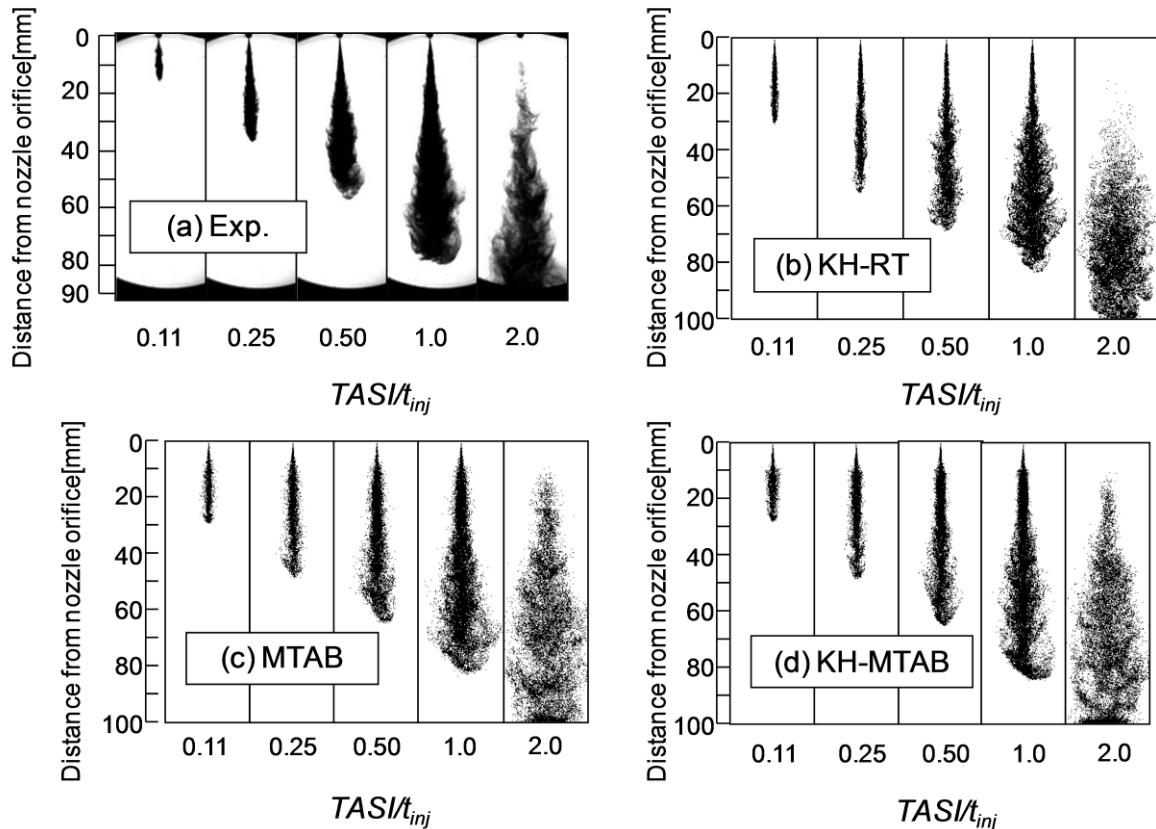


Figure 7 Effects of breakup model on instantaneous spray images as a function of non-dimensional time $TASI/t_{inj}$

Investigation of availability of breakup model at different ambient densities

Figure 8 shows spray image of LES and experimental results at different ambient densities. Experimental images are taken by shadowgraph photography. LES simulated intermittency of spray outline as same as experiment. However, each condition of LES, spread of spray radial directions underestimated at the 10-30mm from the nozzle tip. It does not take into account the excluded volume of the gas phase by droplet, so that the prediction accuracy near the nozzle is low due to a high number density of droplet.

Figure 9 shows the time series of spray tip penetration at different ambient densities. Experiment result is the ensemble average of 10 times from shadowgraph photography. LES was generally consistent with the experimental results in the any ambient density. However, spray tip penetration was overestimated at initial injection that is 0.0-0.5 ms from the start of injection, in the any conditions. This is because, the same reason mentioned earlier, the calculation does not take into account the excluded volume of the gas phase by droplet, so that the prediction accuracy is low and underestimate the spread of spray radial directions at the base of spray.

Figure 10 shows time series of spray volume. Experimental results are the ensemble average of 10 times from shadowgraph photography. LES results were similar to experiment, which reproduce the tendency to increase the spray volume by increasing the injection pressure. Also, LES was only underestimated from the experimental results at an ambient density of 35.5 kg/m³. The radial distance of the spray was presented in figure 11 for consideration of this cause. LES was compared with the experiment from the figure, to be matched qualitatively. The spray volume, however, is to be calculated from the average circumferential direction, which is greatly affected by the maximum radial distance of the spray. Therefore, LES turned out lower than the experimental results. In addition, the rapid increase of spread of spray radial direction can be seen in the region of 0-20mm from the nozzle tip at any conditions due to the switching of the breakup model. In this study, the breakup model is switched across the board when it comes to less than or equal to the Weber number 450, in order to improve the transition region by providing coexist of two models.

LES and experimental results of Particle Distribution frequency (PDF) of entire region of spray by SHSRP in pilot spray condition at $t/t_{inj}=7.0$ are shown in figure 12. PDF result of LES and experiment did not change even if change the ambient densities. However, small droplets are largely existed in LES analysis compared to the experimental results. Also, LES is underestimated the PDF in nearly 20 μ m.

LES and experimental results of SMD of entire region of spray by SHSRP in pilot spray condition at $TASI/t_{inj}=7.0$ are shown in figure 13. LES is underestimated the experimental results. The experimental results with the increase of ambient densities, the SMD decreased, but the LES results had become constant value, does not match the qualitative. This is because SMD is mainly influenced by large droplets. From the figure 12, LES is underestimated at the nearly 20 μ m, compared to experiment.

Consequently, LES is difficult to predict the SMD and PDF at high ambient condition. This is because droplet number density tendency to increase by increasing the ambient density. In this study does not take into account the excluded volume of the gas phase by droplet. Prediction accuracy can be expected to improve by considering the excluded volume.

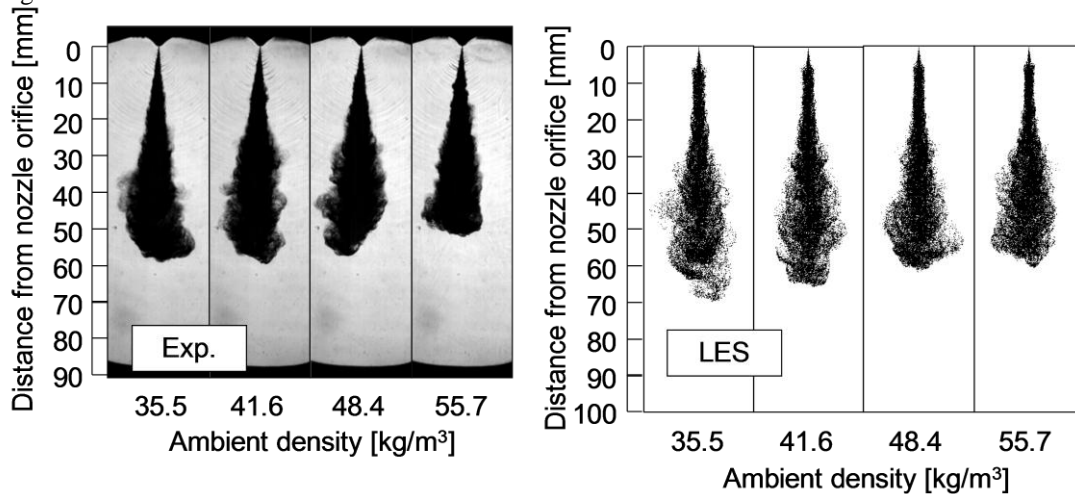


Figure 8 Effect of ambient density on instantaneous spray images at the time of spray injection end (Main injection)

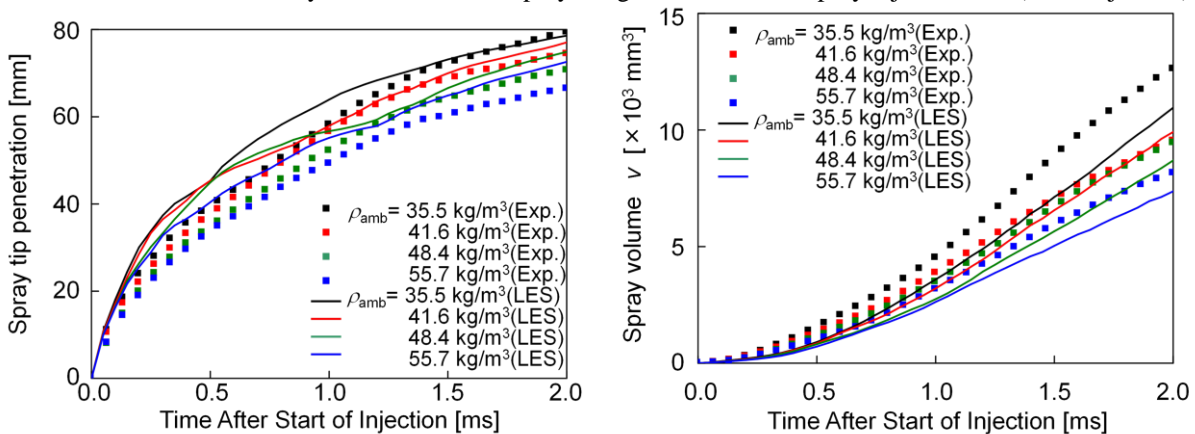


Figure 9 Temporal changes in spray tip penetration as a function of time after start of injection for different ambient density (Main injection)

Figure 10 Temporal changes in spray volume as a function of time after start of injection for different ambient density (Main injection)

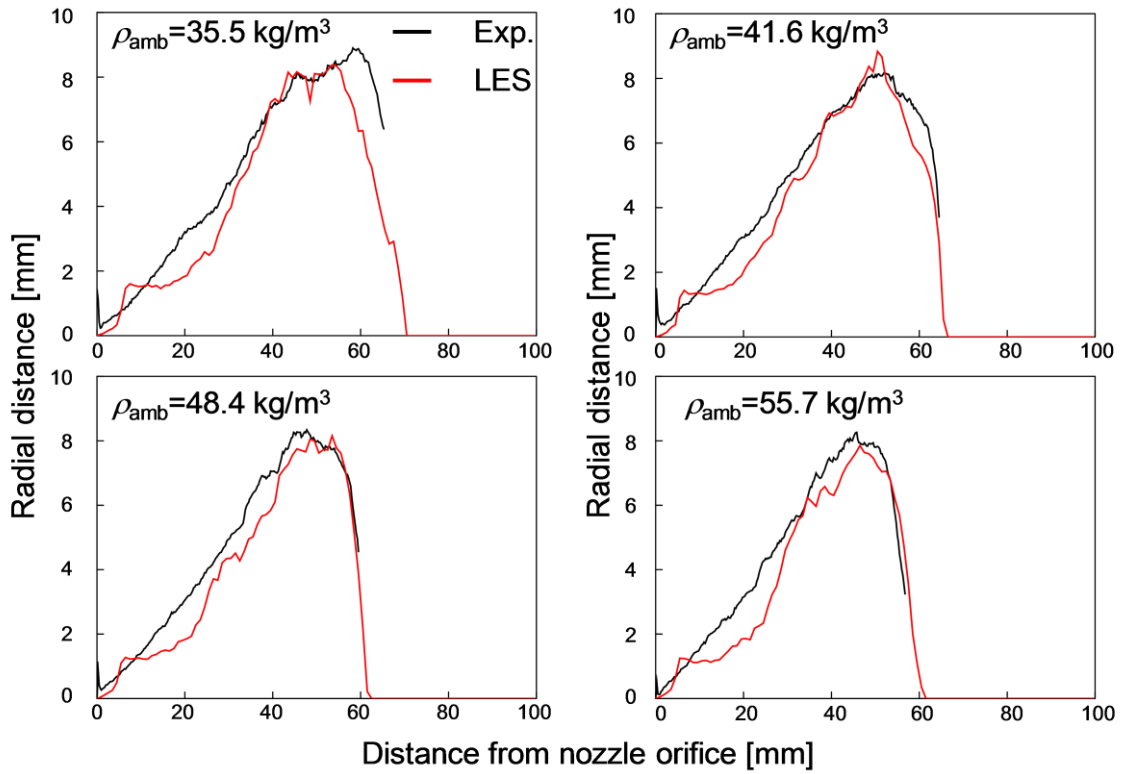


Figure 11 Spray radial distance at the time of injection end (Main injection)

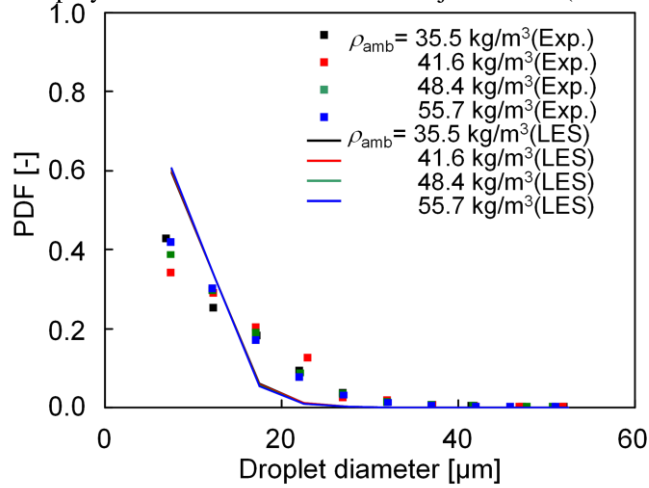


Figure 12 Effects of ambient density probability density function of all spray regions at $TASI/t_{inj}=7.0$ (Pilot injection)

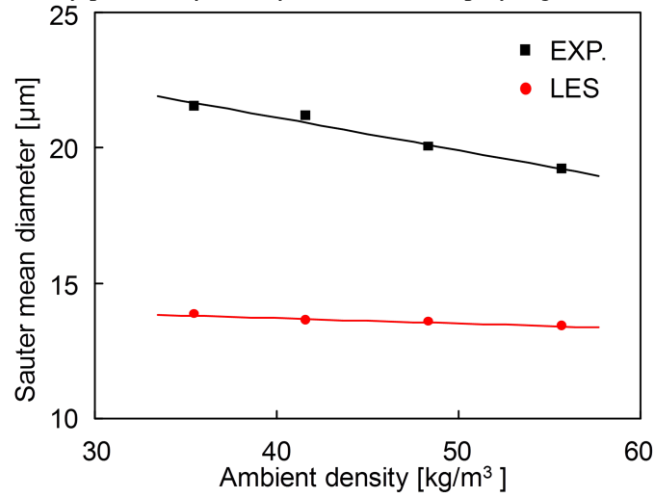


Figure 13 Effects of ambient density sauter mean diameter of all spray regions at $TASI/t_{inj}=7.0$ (Pilot injection)

Summary and Conclusions

This paper shows the study for optimizing the breakup model, calculated non-evaporation spray analysis. First, we examined the effect of breakup model under relatively low density conditions. After that, validation under the ambient density 35.5-55.7 kg/m³ are conducted in order to simulate the injection at the high density of supercharging and high EGR diesel engines. The following conclusions are obtained.

1. In relatively low density conditions, KH-MTAB model can represent spray characteristic than KHRT model and MTAB model.
2. In KH-MTAB model under the ambient density from 35.5 to 55.7 kg/m³, spray tip penetration is generally consistent with the experimental results. In addition, spray volume is in qualitatively agreement with experiment, has decreased with increasing ambient density at conditions change from 35.5 to 55.7 kg/m³.
3. In KH-MTAB model, particle distribution frequency is underestimated the nearly 20μm compared with experiment at high ambient condition. Hence sauter mean diameter is disagreement with experiment.

Acknowledgements

This work was supported by Grants-in-Aid for Scientific Research (B) (17360102). Also, part of this work was supported by "Academic frontier promotion work" of academic research promotion work in private universities by the Ministry of Education, Culture, Sports, Science and Technology, "Next generation zero emission energy conversion system"(S0901038 : 2009-2013).

References

- [1] T. Hori, T. Kuge, J. Senda and H. Fujimoto, "Large Eddy Simulation of Non-Evaporative and Evaporative Diesel Spray in Constant Volume Vessel by Use of KIVALES", SAE Paper 2006-01-3334, 2006.
- [2] H. Fujimoto, T. Hori, J. Senda, "Effect of Breakup Model on Diesel Spray Structure Simulated by Large Eddy Simulation", SAE paper 2009-24-0024, 2009.
- [3] T. Hori, T. Kuge, J. Senda and H. Fujimoto, "Large Eddy Simulation of Diesel Spray Combustion with Eddy-Dissipation Model and CIP Method by Use of KIVALES", SAE paper 2007-01-0247, 2007.
- [4] K. Sone and S. Menon, "Effect of Subgrid Modeling on the In-Cylinder Unsteady Mixing Process in a Direct Injection Engine", J. Eng. Gas Turb. Power, Vol.125, pp.435-443, 2003.
- [5] K. Sone, N. V. Patel and S. Menon, "KIVALES : Large-Eddy simulation of Internal Combustion Engines. Part 1 : Theory and Formulation", Technical Report CCL-00-008, Georgia Institute of Technology, 2000.
- [6] K. Sone, V. N. Patel and S. Menon, "KIVALES : A New Large-Eddy Simulation Approach Based on the Kiva-3V Code. Part 2 : User's Manual", Technical Report CCL-00-009, Georgia Institute of Technology, 2000.
- [7] Amsden and O'Rourke, "KIVA-2 A Computer Program for Chemically Reactive Flows with Sprays", LA-11560-MS, Los Alamos National Laboratory, 1989.
- [8] Alex B. Liu, Daniel Mather and Rolf D. Reitz, "Modeling the Effects of Drop Drag and Breakup on Fuel Sprays", SAE paper No.930072, 1993.
- [9] N. Marubayashi, T. Yano, T. Hori, J. Senda, H. Fujimoto, "Measurement method of digital holography for diesel spray : Construction of filter for reducing noise", Symposium (ILASS-Japan) on Atomization 19, pp.88-92, 2010.
- [10] R. D. Reitz, "Modeling atomization processes in high spray pressure vaporizing sprays", Atomization and Technol., Vol.3, pp.309-337, 1987.
- [11] J. Senda, T. Dan, S. Takagishi, T. Kanda and H. Fujimoto, "Spray characteristics of non-reacting diesel fuel spray by experiments and simulations with KIVA2", Proceedings of ICLASS, 1997.
- [12] P. J. O'Rourke, A. Amsden, "The TAB Method for Numerical Calculation of Spray Drop Breakup", SAE paper, No.872089, 1987.
- [13] V. G. Levich, "Physicochemical Hydrodynamics", Prentice-Hall, Englewood Cliffs, NJ, 1963.
- [14] T. Kamimoto, H. Yokota and H. Kobayashi, "A new technique for the measurement of Sauter mean diameter of droplets in unsteady dense sprays", SAE paper No.890316, 1989.
- [15] T. Dan, J. Senda, "Effect of Ambient Gas Properties for Characteristics of Non-Reacting Diesel Fuel Spray", SAE paper No.970352, 1997.